AD-A036 684 PENNSYLVANIA STATE UNIV UNIVERSITY PARK APPLIED RESE--ETC F/G 20/11
VISCOUSLY DAMPED DYNAMIC ABSORBERS OF CONVENTIONAL AND NOVEL DE--ETC(U)
DEC 76 M A NOBILE, J C SNOWDON N00017-73-C-1418
UNCLASSIFIED TM-76-308 NL

1 OF 1
AD-A
036 684

END
DATE
FILMED
4-1-77
NTIS

VISCOUSLY DAMPED DYNAMIC ABSORBERS OF CONVENTIONAL AND NOVEL DESIGN

PENNSYLVANIA STATE UNIVERSITY
UNIVERSITY PARK

10 DECEMBER 1976

The Pennsylvania State University
Institute for Science and Engineering
APPLIED RESEARCH LABORATORY
Post Office Box 30
State College, Pa. 16801

NAVY DEPARTMENT

NAVAL SEA SYSTEMS COMMAND

VISCOUSLY DAMPED DYNAMIC ABSORBERS OF CONVENTIONAL AND NOVEL DESIGN (U)

M. A. Nobile and J. C. Snowdon

Technical Memorandum
File No. TM 76-308
December 20, 1976
Contract No. N00017-73-C-1418

Copy No. 56

The Pennsylvania State University
Institute for Science and Engineering
APPLIED RESEARCH LABORATORY
Post Office Box 30
State College, PA 16801

NAVY DEPARTMENT

NAVAL SEA SYSTEMS COMMAND

This investigation was sponsored by the Naval Sea Systems Command, Ship Silencing Division, and the Office of Naval Research.

UNCLASSIFIED

SECURITY CLASSIFICATION OF THIS PAGE (When Data Entered)

REPORT DOCUMENTATION PAGE		READ INSTRUCTIONS BEFORE COMPLETING FORM
1. REPORT NUMBER TM 76-308	2. GOVT ACCESSION NO.	3. RECIPIENT'S CATALOG NUMBER
4. TITLE (and Subtitle) Viscously Damped Dynamic Absorbers of Conventional and Novel Design (U)		5. TYPE OF REPORT & PERIOD COVERED 6. PERFORMING ORG. REPORT NUMBER
7. AUTHOR(s) M. A. Nobile and J. C. Snowdon		8. CONTRACT OR GRANT NUMBER(s) N00017-73-C-1418
9. PERFORMING ORGANIZATION NAME AND ADDRESS The Pennsylvania State University Applied Research Laboratory P. O. Box 30, State College, PA 16801		10. PROGRAM ELEMENT, PROJECT, TASK AREA & WORK UNIT NUMBERS SF 43-452-702 (NavSea) N00014-76-RQ-00002 (ONR)
11. CONTROLLING OFFICE NAME AND ADDRESS Naval Sea Systems Command Office of Naval Research Department of the Navy Department of the Navy Washington, DC 20362 Arlington, VA 22217		12. REPORT DATE December 20, 1976 13. NUMBER OF PAGES 52
14. MONITORING AGENCY NAME & ADDRESS(if different from Controlling Office)		15. SECURITY CLASS. (of this report) UNCLASSIFIED 15a. DECLASSIFICATION/DOWNGRADING SCHEDULE

16. DISTRIBUTION STATEMENT (of this Report)

Approved for public release; distribution unlimited.
Per NAVSEA January 21, 1977.

17. DISTRIBUTION STATEMENT (of the abstract entered in Block 20, if different from Report)

18. SUPPLEMENTARY NOTES

19. KEY WORDS (Continue on reverse side if necessary and identify by block number)

Dynamic vibration absorbers.
Vibration isolation.
Viscous damping.
Dashpots.
Transmissibility.

20. ABSTRACT (Continue on reverse side if necessary and identify by block number)

The behavior of dynamic vibration absorbers of conventional and novel design has been investigated experimentally and found to compare closely with prediction. The dynamic absorbers were employed to suppress the transmissibility at resonance across a one-degree-of-freedom primary system. Initially considered was a dynamic absorber with a conventional mass-spring-dashpot configuration; the primary system was undamped. Subsequently considered were (1) so-called dual dynamic absorbers, and (2) a single, nominally undamped

DD FORM 1 JAN 73 1473 EDITION OF 1 NOV 65 IS OBSOLETE

UNCLASSIFIED

SECURITY CLASSIFICATION OF THIS PAGE (When Data Entered)

absorber, or two such absorbers, attached to the primary system after it had been damped heavily.

The dual absorbers -- a conventional viscously damped absorber used in parallel with a less massive undamped absorber -- introduced a pronounced transmissibility trough without the appearance of unwanted "compensating" peaks at lower and higher frequencies. The attachment of a nominally undamped absorber to the heavily damped primary system also introduced a pronounced trough without giving rise to compensating peaks. Further, the attachment of two such absorbers introduced pronounced troughs at two frequencies that could be varied independently of one another. Thus, the novel absorber systems considered here behaved as mechanical "notch" filters, providing at specific "low" frequencies a high degree of isolation that other passive systems cannot duplicate without exhibiting a marked loss in isolation at neighboring frequencies.

ABSTRACT

The behavior of dynamic vibration absorbers of conventional and novel design has been investigated experimentally and found to compare closely with prediction. The dynamic absorbers were employed to suppress the transmissibility at resonance across a one-degree-of-freedom primary system. Initially considered was a dynamic absorber with a conventional mass-spring-dashpot configuration; the primary system was undamped. Subsequently considered were (1) so-called dual dynamic absorbers, and (2) a single, nominally undamped absorber, or two such absorbers, attached to the primary system after it had been damped heavily.

The dual absorbers -- a conventional viscously damped absorber used in parallel with a less massive undamped absorber -- introduced a pronounced transmissibility trough without the appearance of unwanted "compensating" peaks at lower and higher frequencies. The attachment of a nominally undamped absorber to the heavily damped primary system also introduced a pronounced trough without giving rise to compensating peaks. Further, the attachment of two such absorbers introduced pronounced troughs at two frequencies that could be varied independently of one another. Thus, the novel absorber systems considered here behaved as mechanical "notch" filters, providing at specific "low" frequencies a high degree of isolation that other passive systems cannot duplicate without exhibiting a marked loss in isolation at neighboring frequencies.

INTRODUCTION

The conventional dynamic absorber comprises a mass M_2 that is attached via a single spring and damper to a vibrating item of mass M_1, which is excited by a sinusoidally varying force $\tilde{F}_1$, as in Fig. 1(a), or by a sinusoidally varying ground displacement $\tilde{x}_1$, as in Fig. 1(b).[1] In either case, M_1 resonates on resilient members of total stiffness K_1. The mass M_2 is tuned to resonate at a similar frequency at which its motion becomes relatively large, whereas the force $2\tilde{F}_2$ transmitted to the ideally rigid foundation in Fig. 1(a), or the displacement $\tilde{x}_2$ of the vibrating item in Fig. 1(b), is minimized. For an instrument mounting, when M_1 represents an item of electronics, a laser table, etc., M_2 might be equal to M_1; whereas, if M_1 represents a large item of machinery, it is unlikely that M_2 would exceed 20% of M_1.

A quantity of basic interest is the transmissibility T across the systems of Fig. 1. It can be shown[2] that, if the transmissibility across system (a) is defined as the magnitude of the force ratio $|2\tilde{F}_2/\tilde{F}_1|$, and if the transmissibility across system (b) is defined as the magnitude of the displacement ratio $|\tilde{x}_2/\tilde{x}_1|$ or of the acceleration ratio $|\tilde{A}_2/\tilde{A}_1|$ -- then, at any one frequency,

$$T = \left|\frac{2\tilde{F}_2}{\tilde{F}_1}\right| = \left|\frac{\tilde{x}_2}{\tilde{x}_1}\right| = \left|\frac{\tilde{A}_2}{\tilde{A}_1}\right| \quad . \tag{1}$$

In this equation, $\tilde{A}_i = (j\omega)^2\tilde{x}_i$, $i = 1, 2$, where $j = \sqrt{(-1)}$ and ω is angular frequency, hereafter referred to simply as frequency. The results of a single calculation or measurement of transmissibility thus have dual

significance. Consequently, in the experiments to be described here, T has been determined as the readily measurable acceleration ratio $|\tilde{A}_2/\tilde{A}_1|$ rather than as the force ratio $|2\tilde{F}_2/\tilde{F}_1|$, which is more difficult to measure.

The concept of the conventional dynamic absorber was first described in 1928.[3] Since then, much has been written about how the absorber should be tuned and damped; that is, how values of the stiffness K_2 of the absorber spring and the coefficient of viscosity η_2 of the dashpot should be chosen to provide optimum absorber performance. It is an advantage that the optimum values of K_2 and η_2 provide the same optimum absorber performance in both Figs. 1(a) and 1(b). In fact, for a primary system (M_1, K_1) with negligible damping, the optimum values[2] of the absorber tuning ratio $n = (\omega_a/\omega_o)$ and the absorber damping ratio δ_{2R} are

$$n_{opt} = (\omega_a/\omega_o)_{opt} = (\mu)^{\frac{1}{2}} \tag{2}$$

and

$$(\delta_{2R})_{opt} = [3(1 - \mu)/8]^{\frac{1}{2}} \quad , \tag{3}$$

where

$$\omega_a = (K_2/M_2)^{\frac{1}{2}} \tag{4}$$

is the natural frequency of the dynamic absorber,

$$\omega_o = [K_1/(M_1 + M_2)]^{\frac{1}{2}} = (\mu K_1/M_1)^{\frac{1}{2}} \tag{5}$$

is a reference frequency that has been introduced for convenience, and the mass ratio

$$\mu = M_1/(M_1 + M_2) \quad . \tag{6}$$

The damping ratio

$$\delta_{2R} = \eta/\eta_c = \omega_a \eta /2K_2 \quad , \tag{7}$$

where η_c is the value of the coefficient of viscosity required to damp the absorber critically. For example, if $M_2 = M_1/5$, then $\mu = 5/6$, $n_{opt} = 0.913$, and $\delta_{2R} = 0.25$; that is, the absorber should have 25% of critical damping.

The validity of the foregoing expressions has been confirmed by transmissibility measurements that are described here initially. Consideration is given subsequently to dynamic absorbers having novel configurations, the predictions for which have also been confirmed by experiment. These novel configurations comprise (1) a single, nominally undamped absorber,[2] or a pair of such absorbers, attached to a heavily damped primary system, and (2) so-called "dual dynamic absorbers" -- a conventional, viscously damped absorber placed in parallel with a less massive, nominally undamped absorber.[4]

Although the theory of the damped conventional dynamic absorber is well developed, controlled laboratory testing such as that described here has been sparse; in fact, there is a particular lack of experimental data in the prior literature. Exceptions are described in Refs. 5-7, which relate solely to dynamic absorbers with viscoelastic supporting elements. Several noteworthy practical applications of dynamic absorbers are described in Refs. 8-16.

1. NOMINALLY UNDAMPED PRIMARY SYSTEM

The transmissibility across the primary system (M_1, K_1) of Fig. 1 in the absence of the absorber can be expressed as

$$T = \left[\frac{1 + \delta_{1K}^2}{(1 - \Omega^2)^2 + \delta_{1K}^2}\right]^{\frac{1}{2}} \quad . \tag{8}$$

In this equation, δ_{1K} is the small (nominally zero) solid-type damping factor of the supporting springs of stiffness K_1, and the frequency ratio

$$\Omega = \omega/\omega_o \quad , \tag{9}$$

where ω_o currently represents the natural frequency of the system; namely,

$$\omega_o = (K_1/M_1)^{\frac{1}{2}} \quad . \tag{10}$$

At this frequency, for which $\Omega = 1.0$,

$$T = (1 + \delta_{1K}^2)^{\frac{1}{2}}/\delta_{1K} \approx 1/\delta_{1K} \quad , \tag{11}$$

an equation that yields the damping factor of the springs if T is measured at resonance.

As mentioned, the experiments described here related to the system of Fig. 1(b) for which accelerometers attached to M_1 and to the "vibrating foundation" provided the values needed to determine transmissibility directly (Eq. 1). The assembly employed was that shown in Fig. 2, where the foundation was modeled by a 3-in. thick, 19-in. long, slab of aluminum. The primary mass M_1 comprised an inverted-T aluminum structure that weighed approximately 10 lb and that incorporated flanges to provide a base for the absorber dashpots, which will be described later. The supporting springs, of total stiffness K_1, consisted of two identical precision-ground steel strips clamped between the upper and lower sections of M_1. The ends of the steel strips were likewise held by clamps that could be released and moved

to vary the effective length and, hence, the stiffness of the strips, thus providing a means by which the natural frequency ω_o could be varied continuously through a broad range of values. Because electronic equipment limitations dictated a lower bound to the experiments of approximately 9 Hz, and because both the foundation and the primary mass M_1 ceased to vibrate as ideally rigid members at frequencies above 1000 Hz (at higher frequencies, the foundation vibrated essentially as a free-free beam, and the central portion and flanges of M_1 vibrated with different phase), measurements were made through the two-decade range 9 - 900 Hz with the resonant frequency $\omega_o/2\pi$ set at approximately 90 Hz.

The foundation and primary mass, and a central vibration generator rated to deliver 50-lb peak force, were supported by a concrete seismic mass, as shown in Fig. 3. The seismic mass, which weighed 800 lb, was resiliently mounted with a vertical natural frequency of 9 Hz on a concrete base block. The static load of the test apparatus was decoupled from the vibration generator by soft rubber foundation mounts. After preamplification, signals from accelerometers mounted on M_1 and the foundation were channeled via a tracking filter either to a voltmeter or to an automatic level recorder. The accelerometer-preamplifier combinations were adjusted to have identical sensitivities.

That the primary mass M_1 and the steel-strip springs K_1 did behave as a single-degree-of-freedom system is confirmed by the measured results, which are plotted in Fig. 4 as a function of the frequency ratio $\Omega = \omega/\omega_o$, where $\omega_o/2\pi = 90.5$ Hz. Transmissibility takes the value unity at low frequencies and diminishes at 12dB/octave at high frequencies, as predicted. The measured peak height of 44.4 dB indicates that the effective internal damping factor of the steel-strip springs was $\delta_{1K} = 0.006$.

2. CONVENTIONAL DYNAMIC ABSORBER

The transmissibility across the dynamic absorber systems of Fig. 1 is given[2] by

$$T = [(\Omega^2 - n^2)^2 + (2n\Omega\delta_{2R})^2]^{\frac{1}{2}}/\Psi \quad , \tag{12}$$

where

$$\Psi = \{[\mu\Omega^4 - \Omega^2(1 + n^2) + n^2]^2 + (2n\Omega\delta_{2R})^2(\Omega^2 - 1)^2\}^{\frac{1}{2}} \tag{13}$$

and where $\Omega = \omega/\omega_o$ is now rephrased in terms of the reference frequency ω_o specified by Eq. 5. In practice, the relative displacement between the primary and absorber masses is also of interest because it provides a measure of the stress in the absorber spring that connects M_2 to M_1. (The relative displacement increases as M_2 decreases in comparison to M_1, and it is important that the corresponding stress does not become excessive.) The normalized relative displacement -- henceforth, the relative displacement RD -- is simply given by

$$RD = |(\tilde{x}_3 - \tilde{x}_2)/\tilde{x}_1| = \Omega^2/\Psi \quad , \tag{14}$$

where $\tilde{x}_3$ is the displacement of M_2.

Experimentally, the design requirements were (1) that the absorber mass and supporting spring comprise a one-degree-of-freedom system throughout the frequency range of interest, and (2) that the stiffness of the spring -- and, hence, the resonant frequency of the absorber -- be continuously variable to facilitate absorber tuning. Thus, precision-ground steel strips were again chosen for the springs, and the absorber mass was designed so

that it could be arbitrarily located along them. Because it was desired to preserve symmetry to avoid possible rocking motion of the primary system, the absorber took the form of the double cantilever shown in Fig. 5(a), where the total absorber mass and stiffness are M_2 and K_2.

Each absorber mass ($M_2/2$) consisted of two cylindrical steel discs that were bolted together to "sandwich" the steel-strip spring rigidly. A milled guide slot in the lower disc enabled the absorber mass to be accurately positioned. The total mass of the absorber elements was exactly one-fifth of the primary mass, so that $\mu = M_1/(M_1 + M_2) = 5/6$.

Piston-in-cylinder dashpots beneath each mass $M_2/2$ supplied absorber damping as indicated in Figs. 5(b) and 5(c). The prime requirement that the coefficient of viscosity η of the dashpot -- and thus the damping ratio δ_{2R} -- be continuously variable was satisfied in two ways. First, for a coarse variation of damping, the viscosity of the silicone fluid in the cylinder was changed and, second, for a fine variation, the piston was raised or lowered slightly. Thus, a threaded stud, rigidly attached to the piston, could be rotated into the absorber mass to change the immersed depth of the piston and the resultant viscous drag. The dashpot cylinders were fastened to the primary mass with clamps, which could be released to allow the cylinders to be repositioned when the location of the absorber masses, and hence, the tuning of the absorber, was varied. Because the piston and cylinder masses contributed directly to M_2 and M_1, they were designed carefully to preserve the value of the mass ratio $\mu = 5/6$, for which the damping ratio $(\delta_{2R})_{opt} = (\eta/\eta_c)_{opt} = 0.25$.

For any required value of δ_{2R}, the appropriate viscosity of the dashpot fluid was determined[17] from the formula

$$\eta = 6\pi\mu_a \ell (a/t)^3 [1 + 1.5(t/a)] \quad , \tag{15}$$

where μ_a is the absolute fluid viscosity, ℓ is the immersed depth of the piston, a is the piston radius, and t is the piston-to-cylinder clearance [nb, absolute viscosity (cp) = kinematic viscosity (cs) x fluid density (gm/cm^3)]. The simpler and more familiar formula[18]

$$\eta = 6\pi\mu_a \ell (a/t)^3 \tag{16}$$

pertains when (t/a) is small.

Transmissibility measurements ($\mu = 5/6$) were obtained by the method described in Sec. 1, where accelerometers mounted on the foundation and primary mass recorded values of $\tilde{A}_1$ and $\tilde{A}_2$, respectively. In addition, matched accelerometers now recorded the acceleration $\tilde{A}_3$ of the absorber masses $M_2/2$. Here, and subsequently, the reference frequency was $\omega_o/2\pi = 82.5$ Hz. The viscosity of the dashpot fluid and the depth of immersion of the pistons in the dashpots were assigned the values predicted by Eq. 15 to yield optimum absorber damping. This formula proved remarkably accurate, and only slight alterations of the piston setting were necessary to achieve $(\delta_{2R})_{opt}$ precisely. (For dashpots with $\ell = 0.42$ in., a = 0.625 in., and t = 0.0625 in., as utilized here, a fluid viscosity of 500 cs provided optimum damping.) The absorber tuning ratio was set to its predicted optimum value of $n_{opt} = \sqrt{\mu} = 0.913$; consequently, $\omega_2/2\pi = 75.31$ Hz. Compensating transmissibility peaks[2] of slightly different height then resulted. Accordingly, the tuning ratio was varied ($\omega_2/2\pi \rightarrow 80.83$ Hz) until equal maxima were obtained. This change was perhaps necessary because the effective mass of M_2 was increased and, hence, the resonant frequency of the absorber decreased by the presence of the high-viscosity dashpot fluid. (When the absorber was undamped, the predicted tuning ratio yielded results in close accord with theory.)

The measured transmissibility $T = |\tilde{A}_2/\tilde{A}_1|$ across the damped absorber system is plotted in Fig. 6 versus the frequency ratio $\Omega = \omega/\omega_o$. Again, these results are in close accord with theory[2] because the measured values of the transmissibility maxima, and of the intervening minimum, 10.5 and 8.9 dB, respectively, agree well with their predicted values of 10.4 and 9.3 dB; in addition, as predicted at higher frequencies, the effect of the absorber diminishes and the transmissibility curve falls off at the same rate of 12 dB/octave as the transmissibility across the primary system alone.

It is readily apparent from Fig. 6 that the optimally tuned and damped dynamic absorber is a most effective device for vibration control. Whereas the primary system exhibited a resonant amplification of 44.4 dB, the addition of the absorber ($\mu = 5/6$) has reduced this value to 10.5 dB; that is, transmissibility has been reduced by a factor of 50.

The associated relative displacement RD (Eq. 14) across the absorber spring is plotted in Fig. 7. Thus, the relevant accelerations $\tilde{A}_3$ and $\tilde{A}_2$ of the masses M_2 and M_1 were subtracted vectorially by a simple operational amplifier circuit so that $RD = |(\tilde{A}_3 - \tilde{A}_2)/\tilde{A}_1|$ could be determined readily. The relative displacement curve agrees well with prediction,[2] and the observed maximum of 15.5 dB lies 0.3 dB below its calculated value. In turn, this maximum lies some 29 dB below the value of RD_{max} measured when the absorber was undamped, which means that the likelihood of excessive stress in the absorber spring has been reduced significantly.

3. DYNAMIC ABSORBERS ATTACHED TO A HEAVILY DAMPED PRIMARY SYSTEM

It has been demonstrated in the foregoing that a judiciously tuned and damped dynamic absorber can successfully reduce the large transmitted forces and displacements that are generated at the resonance of a nominally

undamped primary system. Characteristically large values of damping in the absorber system are required to suppress the two compensating transmissibility peaks that are introduced by the attachment of the absorber. Unfortunately, damping reduces the depth of the intervening trough to a level only slightly below that of the peaks. It will now be shown that a trough of significant depth can be generated by a nominally undamped absorber, without the introduction of compensating peaks, provided that the primary system can be heavily damped. Although the addition of damping to the system will not always be feasible, it may well be so for an instrument mounting when it is desired to attenuate ground vibration of discrete "low" frequency. Thus, at the frequency of concern, the absorber system will behave as a mechanical "notch filter," providing a high degree of isolation.

A viscously damped primary system and a nominally undamped dynamic absorber are shown in Fig. 8(a). The absorber mass M_2 is suspended from a linear spring of stiffness K_2 having a small (nominally zero) solid-type damping factor δ_{2K}. The primary mass M_1 is supported by springs of total stiffness K_1 and dashpots having a total coefficient of viscosity η_1 for which a viscous damping ratio δ_{1R} is conveniently defined as

$$\delta_{1R} = (\omega_o \eta_1 / 2K_1) \quad . \tag{17}$$

The transmissibility across the system of Fig. 8(a) can be stated[2] as follows:

$$T = [(R_N^2 + I_N^2)/(R_D^2 + I_D^2)]^{\frac{1}{2}} \quad , \tag{18}$$

where

$$R_N = [(n^2 - \Omega^2) - 2\Omega n^2 \delta_{1R}\delta_{2K}] \quad , \tag{19}$$

$$I_N = [n^2\delta_{2K} + 2\Omega\delta_{1R}(n^2 - \Omega^2)] \quad , \tag{20}$$

$$R_D = [\mu\Omega^4 - \Omega^2(1 + n^2) + n^2 - 2\Omega n^2 \delta_{1R}\delta_{2K}] \quad , \tag{21}$$

and

$$I_D = [n^2\delta_{2K}(1 - \Omega^2) + 2\Omega\delta_{1R}(n^2 - \Omega^2)] \quad . \tag{22}$$

The frequency ratio Ω and the tuning ratio n are again defined as in Sec. 2. Representative calculations of transmissibility made from Eq. 18 are plotted in Fig. 9 for an absorber system with a mass ratio $\mu = 5/6$, a damping factor $\delta_{2K} = 0.003$, and a damping ratio $\delta_{1R} = 0.5$ (50% of critical damping). The tuning ratio takes the successive values $n = \omega_a/\omega_o = 0.667$, 1.0, and 1.5. It is apparent that a sharp minimum, indicating desired attenuation, has been introduced at each frequency to which the absorber is tuned, and that unwanted peaks have been avoided. In fact, the maximum values of transmissibility are comparable to the maximum value observed in the absence of the absorber ($T_{max} = 3.33$ dB). When $n = \Omega = 1.0$, the predicted relative displacement RD (Eq. 14) across the absorber spring in Fig. 8(a) is 18.4 dB, a value that is 2.6 dB above the maximum level predicted for the viscously damped absorber in Sec. 2.

Verification of the preceding theoretical results required that the primary system be damped heavily. This was achieved by means of a piston that was attached centrally to the underside of the primary mass M_1, and that protruded into a cylindrical recess in the foundation of Fig. 3, thus forming a conventional dashpot. The recess, 1.75 in. in diameter and 1.0-in. deep, provided a piston clearance t = 1/16 in. The depth of

immersion of the piston could be adjusted by a threaded-stud mechanism similar to that described in Sec. 2. Since 50% of critical damping was sought, a silicone fluid having a viscosity of approximately 3000 cs was used in the dashpot according to the requirements of Eq. 15. The only absorber damping present was that inherent to the steel springs of total stiffness K_2 [Fig. 8(a)].

Measurements were first made of the transmissibility across the one-degree-of-freedom system comprising M_1, K_1, and the primary mass dashpot. The depth of immersion of the piston was adjusted until the maximum transmissibility attained the theoretical value of T_{max} = 3.33 dB, thus assuring that the damping ratio of the primary system was actually δ_{1R} = 0.5 as required. The nominally undamped absorber was then attached to M_1 and the absorber masses were positioned on the steel-strip springs K_2 to yield the required tuning ratios $n = \omega_a/\omega_o$.

The measured transmissibility across the entire system is plotted versus Ω in Fig. 10 for the successive values of n = 0.645, 1.0, and 1.5. These data are in close agreement with the predicted curves of Fig. 9. Agreement between the depths of the troughs in the two figures is not precise because the actual value of the absorber damping factor differed slightly from the representative value of δ_{2K} = 0.003 assumed theoretically (the depths of the troughs are essentially proportional to δ_{2K} when the damping factor is small). The viscous damping force exerted by the dashpot was less than that predicted by Newton's law at high frequencies, where transmissibility diminishes at approximately 10 dB/octave rather than at 6 dB/octave; however, to achieve such an increased rate of attenuation is clearly advantageous.

The companion relative displacement RD across the absorber spring was measured when n = 1.0, and close agreement with theory was again

noted. The value of RD_{max} = 17.2 dB recorded when Ω = 1.0 compared well with the predicted value of 18.4 dB.

It is natural to question whether several independent troughs could be introduced simultaneously into the transmissibility curve by utilizing two or more absorbers tuned to different frequencies. Indeed, as shown here theoretically and confirmed experimentally, two such troughs can be introduced by two absorbers -- and, from these and prior results,[19] it can be expected that any sensible number of troughs can be generated by the use of a like number of absorbers.

A heavily damped primary system to which two nominally undamped dynamic absorbers are attached is shown in Fig. 8(b). The absorbers are assumed to be equally massive ($M_2 = M_3$) and to have springs of different stiffnesses K_2 and K_3 but equal solid-type damping factors $\delta_{2K} = \delta_{3K} = \delta_K$. Because the primary system is again viscously damped, use of the damping ratio δ_{1R} of Eq. 17 remains appropriate. The relevant transmissibility is again given by Eq. 18, where now

$$R_N = [\psi_R - (2\Omega\delta_{1R})\psi_I] \quad , \tag{23}$$

$$I_N = [(2\Omega\delta_{1R})\psi_R + \psi_I] \quad , \tag{24}$$

$$R_D = [R_N - \mu_p\Omega^6 + \chi - \Omega^2(1 - \delta_K^2)n_2^2n_3^2] \quad , \tag{25}$$

and

$$I_D = [I_N + \delta_K(\chi - 2\Omega^2n_2^2n_3^2)] \quad . \tag{26}$$

In these equations

$$\chi = (1 + \mu_p)(n_2^2 + n_3^2)\Omega^4/2 \quad , \tag{27}$$

$$\psi_R = [\Omega^4 - \Omega^2(n_2^2 + n_3^2) + n_2^2 n_3^2 (1 - \delta_K^2)] \quad , \tag{28}$$

$$\psi_I = \delta_K [2n_2^2 n_3^2 - \Omega^2(n_2^2 + n_3^2)] \quad , \tag{29}$$

$$n_2 = \omega_{a2}/\omega_o \quad , \tag{30}$$

$$n_3 = \omega_{a3}/\omega_o \quad , \tag{31}$$

and

$$\mu_p = M_1/(M_1 + 2M_2) \quad , \tag{32}$$

where

$$\omega_{a2} = (K_2/M_2)^{\frac{1}{2}} \quad , \tag{33}$$

$$\omega_{a3} = (K_3/M_3)^{\frac{1}{2}} \quad , \tag{34}$$

and

$$\omega_o = [K_1/(M_1 + 2M_2)]^{\frac{1}{2}} \quad . \tag{35}$$

The results of representative calculations of transmissibility are plotted versus $\Omega = \omega/\omega_o$ in Fig. 11, where M_2 and M_3 are each one-fifth as massive as M_1 ($\mu_p = 5/7$), the damping ratio $\delta_{1R} = 0.5$, the absorber damping factors $\delta_K = 0.002$, and the tuning ratios $n_2 = 1.0$ and $n_3 = 1.5$. It is evident that troughs appear at the frequencies to which the absorbers are tuned, and that the absorbers indeed behave as though they are uncoupled. The depths of the troughs are again essentially proportional to δ_K provided that δ_K remains small.

Experimentally, the addition of a second dynamic absorber to the test apparatus required that the primary mass M_1 be modified. The perpendicular

arrangement of double-cantilever absorbers that was adopted is shown in Fig. 12. Because this arrangement maintained symmetry about the central vertical axis of M_1, rocking motion of the system was avoided. The masses $M_2 = M_3 = 0.2\ M_1$ could be located anywhere along the steel-strip springs of stiffnesses K_2 and K_3, thus permitting the absorber frequencies ω_{a2} and ω_{a3} to be varied continuously, as before. The measured transmissibility across the system is plotted versus Ω in Figs. 13 and 14. Here the absorbers were tuned such that $n_2 = 1.0$ and $n_3 = 1.5$, and $n_2 = 0.667$ and $n_3 = 1.0$, respectively. The damping factors were small ($\delta_K \approx 0.002$) and, as assumed theoretically, $\mu_P = 5/7$ and $\delta_{1R} = 0.5$. The curves of Figs. 13 and 14 correlate closely with prediction. Only a small difference (≈ 0.5 dB) exists between the measured and predicted depths of the troughs because the actual damping factor of the absorber springs was not precisely equal to the assumed value of $\delta_K = 0.002$; however, the relative depths of each pair of troughs closely matched prediction.

4. DUAL DYNAMIC ABSORBERS

It has been confirmed in the foregoing that pronounced minima in transmissibility can be generated without the appearance of the compensating peaks that usually accompany the use of undamped dynamic absorbers. However, the primary system has first to be damped heavily, a requirement that cannot always be satisfied in practice. Consequently, it is natural to question whether a significant trough, without compensating peaks, could also be generated in the transmissibility across an undamped primary system. That this can, in fact, be accomplished by the use of so-called dual dynamic absorbers[4] is now illustrated.

An undamped primary system (M_1, K_1) is shown in Fig. 15, where a conventional viscously damped absorber (M_2, K_2) is attached to M_1 in parallel

with an absorber of mass M_3, which is suspended from M_1 by a spring of stiffness K_3 having a small (nominally zero) solid-type damping factor δ_{3K}. The mass M_3 is assumed to be small in comparison to M_1 and M_2, so that it is again appropriate to define, as in Sec. 2, a reference frequency $\omega_o = [K_1/(M_1 + M_2)]^{\frac{1}{2}}$ and a mass ratio $\mu = M_1/(M_1 + M_2)$. If an additional mass ratio is defined as

$$\beta = M_3/M_2 \quad , \tag{36}$$

and if the nominally undamped absorber is tuned directly to the reference frequency ω_o, that is, if

$$n_3 = \omega_{a3}/\omega_o = \sqrt{(K_3/M_3)}/\omega_o = 1.0 \quad , \tag{37}$$

then transmissibility can again be written as in Eq. 18 where now

$$R_N = [(\varepsilon\mu - \Omega^2)(1 - \Omega^2) - \xi\delta_{3K}] \quad , \tag{38}$$

$$I_N = [\xi(1 - \Omega^2) + \delta_{3K}(\varepsilon\mu - \Omega^2)] \quad , \tag{39}$$

$$\begin{aligned} R_D = \{&-\mu\Omega^6 + \Omega^4[1 + \beta(1 - \mu) + \mu(\varepsilon + 1)] \\ &-\Omega^2\lambda_1[1 + \beta(1 - \mu)] - \Omega^2(\varepsilon\mu + 1) + \lambda_1\} \quad , \end{aligned} \tag{40}$$

and

$$\begin{aligned} I_D = \{&\Omega^4[\xi + \mu\delta_{3K} + \beta\delta_{3K}(1 - \mu)] - \Omega^2\lambda_2[1 + \beta(1 - \mu)] \\ &-\Omega^2(\xi + \delta_{3K}) + \lambda_2\} \quad . \end{aligned} \tag{41}$$

In these equations, ε is a multiplicative constant, and

$$\xi = 2\sqrt{(\varepsilon\mu)}\Omega\delta_{2R} \quad , \tag{42}$$

$$\lambda_1 = (\varepsilon\mu - \xi\delta_{3K}) \quad , \tag{43}$$

and

$$\lambda_2 = (\xi + \varepsilon\mu\delta_{3K}) \quad . \tag{44}$$

Values of the damping ratio δ_{2R} are taken to be those specified by Eq. 3 as optimum for the conventional viscously damped absorber. For each value of δ_{2R}, the parameter ε is adjusted until the optimum absorber tuning ratio

$$(n_2)_{opt} = (\omega_{a2}/\omega_o)_{opt} = \sqrt{(\varepsilon\mu)} \tag{45}$$

yields equal maxima in the resultant transmissibility curve. For example, $\varepsilon = 0.947$ when $\mu = 5/6$, $\beta = \delta_{2R} = 0.25$, and $\delta_{3K} = 0.002$; thus, the appropriate tuning ratio is $(n_2)_{opt} = 0.888$. This value differs only slightly from the value of $n_{opt} = \sqrt{\mu} = 0.913$ specified in Sec. 1 for the conventional absorber alone.

The transmissibility across the dual dynamic absorber system of Fig. 15 has been calculated from Eqs. 18 and 38-44 for the foregoing values of $\mu = 5/6$, $\beta = \delta_{2R} = 0.25$, $\varepsilon = 0.947$, $(n_2)_{opt} = 0.888$, and $\delta_{3K} = 0.002$. The results are plotted versus the frequency ratio Ω in Fig. 16, where the transmissibility maxima share the common value $T_{max} = 11.76$ dB, and the depth of the pronounced trough is $T_{min} = -26.5$ dB. Comparison with the transmissibility of the optimally tuned and damped conventional absorber (Ref. 2 and Fig. 6) shows that the addition of the second, virtually undamped, absorber has reduced T_{min} by essentially 36 dB, whereas T_{max} has been increased by little more than 1 dB. It is an advantage that, in

practice, the second absorber would introduce negligible additional mass and would be easy to apply and simple to tune.

The dual dynamic absorbers were utilized experimentally with the modified primary mass and with the perpendicular double-cantilever configuration shown in Fig. 12. Now, one absorber (M_2, K_2) was replaced by the viscously damped absorber used in the experiments described in Sec. 2, and the second nominally undamped absorber (M_3, K_3) incorporated a different pair of masses to provide the desired mass ratio $\beta = M_3/M_2 = 0.25$. No other changes were required. (An arrangement of two <u>parallel</u> double-cantilever absorbers proved to be unsatisfactory because $M_3 \neq M_2$, and symmetry about the central vertical axis of the primary mass M_1 was not maintained. As a result, a spurious rocking motion of M_1 was introduced near the frequency ω_o by the mass unbalance.)

To measure transmissibility, the masses $M_3/2$ were positioned so that $n_3 = \omega_{a3}/\omega_o = 1.0$; the dashpots of the viscously damped absorber were adjusted to provide the damping ratio $\delta_{2R} = 0.25$; and the positions of the masses $M_2/2$ were varied in unison until equal transmissibility maxima were obtained. At this desired setting of the masses, the damped absorber resonated at a slightly higher frequency than that specified by Eq. 45 [$\omega_{a2} = \sqrt{(\varepsilon\mu)}\omega_o$]. However, it should be recalled that the conventional viscously damped absorber in Sec. 2 likewise had to be tuned to a slightly higher frequency than that specified by Eq. 2 ($\omega_a = \sqrt{\mu}\ \omega_o$). As a consequence, the predicted value of the <u>ratio</u> $\omega_{a2}/\omega_a = \sqrt{\varepsilon} = 0.973$ was actually matched accurately by the value of 0.970 established here by experiment.

The measured transmissibility across the dual absorber system of Fig. 15 is plotted in the final Fig. 17, which exhibits excellent agreement with theory. Thus, the two maxima share a common value of $T_{max} = 12.1$ dB that exceeds prediction by only 0.34 dB, while the intervening trough is

most pronounced, having a measured depth of - 27.1 dB. Further, this trough would be deepened, for example, by 6 dB if δ_{3K} were halved or β were doubled.[4] At high frequencies, transmissibility decreases essentially at 12 dB/octave, as predicted. In fact, these experimental data verify the excellent performance described earlier in this Section for the dual absorber system.

ACKNOWLEDGMENTS

Grateful acknowledgment is made of the help of Adah A. Wolfe in computing the theoretical curves of this paper, and of George E. Norton in constructing the test apparatus. Samples of silicone fluid were provided by the Dow Corning Corporation. The investigation was sponsored by the U. S. Naval Sea Systems Command and the U. S. Office of Naval Research.

REFERENCES

*This paper is based on research conducted by M. A. Nobile in partial fulfillment of the requirements for the M. S. Degree in Engineering Acoustics at The Pennsylvania State University.

1. Symbols with a superior tilde denote sinusoidally varying quantities; symbols with a star superscript denote complex quantities.

2. J. C. Snowdon, Vibration and Shock in Damped Mechanical Systems (John Wiley and Sons, Inc., New York, 1968).

3. J. Ormondroyd and J. P. Den Hartog, "The Theory of the Dynamic Vibration Absorber," Trans. ASME 50, A9 - A22 (1928).

4. J. C. Snowdon, "Dynamic Vibration Absorbers that Have Increased Effectiveness," J. Engr. Ind., Trans. ASME, Ser. B, 96, 940-945 (1974).

5. D. I. G. Jones, A. D. Nashif, and R. L. Adkins, "Effect of Tuned Dampers on Vibrations of Simple Structures," J. AIAA 5, 310-315 (1967).

6. B. J. Stone and C. Andrew, "Optimization of Vibration Absorbers: Application to Complex Structures," J. Mech. Eng. Sci. 11, 221-232 (1969).

7. S. Hahold and K.-P. Schmidt, "Die Unterdrückung von Stab-Eigenschwingungen Durch Schwingungstilger," Acustica 25, 81-88 (1971).

8. D. B. Shotwell, "Application of the Tuned and Damped Dynamic Absorber to Rubber-Tired Earthmoving Machines," ASME Reprint 67-VIBR-64 (1967).

9. P. H. Allaway and P. Grootenhuis, "Unusual Techniques for the Control of Structural Vibration," Paper L36 in Proc. Fifth Intern. Congr. Acoust., Liege (Fifth ICA Committee, Liege, 1965), Pt. 1(b).

10. R. H. Bennett, Jr., and J. D. Van Dyke, Jr., "Aircraft Cabin Noise Reduction System with Tuned Vibration Absorbers," U. S. Patent 3,490,556, Jan. 20, 1970.

11. J. J. O'Leary, "Reduction in Vibration of the CH-47C Helicopter Using a Variable Tuning Vibration Absorber," Shock. Vib. Bull., 40, Pt. 5, 191-202 (1969).

12. M. M. Sadek and S. A. Tobias, "Reduction of Machine Tool Vibration," contribution to Isolation of Mechanical Vibration, Impact, and Noise, J. C. Snowdon and E. E. Ungar, Eds., (ASME Monograph, AMD-1, American Society of Mechanical Engineers, New York, 1973) Chap. 6, pp. 128-172.

13. R. H. Scanlan and R. L. Wardlaw, "Reduction of Flow-Induced Structural Vibrations," contribution to Isolation of Mechanical Vibration, Impact, and Noise, J. C. Snowdon and E. E. Ungar, Eds., (ASME Monograph, AMD-1, American Society of Mechanical Engineers, New York, 1973) Chap. 2, pp. 35-53.

14. R. L. Wardlaw and K. R. Cooper, "Mechanisms and Alleviation of Wind-Induced Structural Vibrations," Proc. 2nd. Symposium Applications of Solid Mechanics (Faculty of Engineering, McMaster Univ., Hamilton, Ont., Canada, 1974), pp. 369-399.

15. Anon., "Dampers May Stop Bridge Vibration," Eng. News Recd. 195, No. 13, 16 (1975).

16. J. D. Raynesford, "Use Dynamic Absorbers to Reduce Vibration," Hydrocarbon Processing 54, 167-71 (1975).

17. D. A. Harding, "Dashpot Coefficients -- Use with Large Clearances," correspondence with J. C. Snowdon (1960).

18. J. B. Peterson, "Damping Characteristics of Dashpots," Natl. Adv. Comm. Aeron., Tech. Note No. 830 (1941).

19. J. C. Snowdon,"Steady-State Behavior of the Dynamic Absorber -- Addendum," J. Acoust. Soc. Am. 36, 1121-1123 (1964).

FIGURE LEGENDS

Fig. 1 Undamped primary system with springs of total stiffness K_1 and with a mass M_1 to which a viscously damped vibration absorber is attached.

Fig. 2 Experimental design of the primary system and its foundation. End clamps can be adjusted to vary the stiffness K_1 of the steel-strip springs and, hence, the resonant frequency of the primary system.

Fig. 3 Test apparatus mounted on a steel-surfaced seismic mass to which foundation support pillars and the housing of a vibration generator are bolted.

Fig. 4 Measured transmissibility across the primary system (M_1, K_1) of Fig. 1(b) plotted versus the frequency ratio $\Omega = \omega/\omega_o$.

Fig. 5 (a) Double cantilever dynamic vibration absorber attached to the primary mass M_1, (b) partial view of a dashpot cylinder located beneath one absorber mass $M_2/2$, and (c) cross-sectional view of the piston-in-cylinder dashpots that damp the dynamic absorber viscously.

Fig. 6 Measured transmissibility across the viscously damped dynamic absorber system of Fig. 1(b) when the mass ratio $\mu = M_1/(M_1 + M_2) = 5/6$; the absorber is judiciously tuned and damped [tuning and damping ratios $n_{opt} \approx \sqrt{\mu}$ and $(\delta_{2R})_{opt} = 0.25$].

Fig. 7 Measured relative displacement across the viscously damped dynamic absorber of Fig. 1(b) when $\mu = 5/6$ and the absorber is tuned and damped as in Fig. 6.

Fig. 8 (a) Nominally undamped dynamic absorber, and (b) a pair of nominally undamped dynamic absorbers attached to a viscously damped primary system having a damping ratio δ_{1R}.

Fig. 9 Calculated transmissibility across the system of Fig. 8(a) when $\mu = 5/6$ and the absorber tuning ratio takes the successive values $n = 0.667$, 1.0, and 1.5. The damping ratio $\delta_{1R} = 0.5$, and the solid-type damping factor of the absorber $\delta_{2K} = 0.003$.

Fig. 10 Measured transmissibility across the system of Fig. 8(a) when $\mu = 5/6$, $\delta_{1R} = 0.5$, and the absorber tuning ratio takes the successive values $n = 0.645$, 1.0, and 1.5.

Fig. 11 Calculated transmissibility across the system of Fig. 8(b) when the mass ratio $\mu_P = 5/7$ ($M_2 = M_3 = 0.2\ M_1$), $\delta_{1R} = 0.5$, and $\delta_K = 0.002$. The absorber tuning ratios $n_2 = 1.0$ and $n_3 = 1.5$.

Fig. 12 Experimental design of the modified primary mass to which a pair of double-cantilever dynamic vibration absorbers is attached.

Fig. 13 Measured transmissibility across the system of Fig. 8(b) when $\mu_P = 5/7$, $\delta_{1R} = 0.5$, and the absorber tuning ratios $n_2 = 1.0$ and $n_3 = 1.5$.

Fig. 14 Measured transmissibility across the system of Fig. 8(b) when $\mu_P = 5/7$, $\delta_{1R} = 0.5$, and the absorber tuning ratios $n_2 = 0.667$ and $n_3 = 1.0$.

Fig. 15 Undamped primary system to which dual dynamic absorbers are attached. The conventional dynamic absorber of mass M_2 is viscously damped; the absorber of small mass M_3 is nominally undamped.

Fig. 16 Calculated transmissibility across the system of Fig. 15 when $\mu = 5/6$ and $\beta = M_3/M_2 = 0.25$. The dynamic absorber of mass M_2 is optimally tuned and damped; the absorber of mass M_3 has a tuning ratio $n_3 = 1.0$ and a solid-type damping factor $\delta_{3K} = 0.002$.

Fig. 17 Measured transmissibility across the system of Fig. 15 when $\mu = 5/6$, $\beta = 0.25$, and $n_3 = 1.0$. The dynamic absorber of mass M_2 is judiciously tuned and damped [$(n_2)_{opt} \approx \sqrt{\varepsilon\mu}$ and $\delta_{2R} = 0.25$].

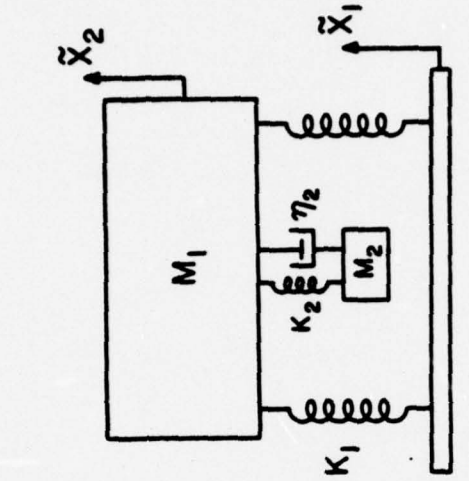
$\tilde{X}_2$
$\tilde{X}_1$
M_1
η_2
M_2
K_2
K_1

(b)

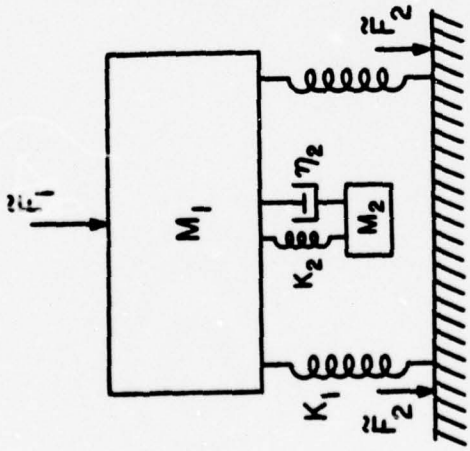
$\tilde{F}_2$
$\tilde{F}_1$
M_1
η_2
M_2
K_2
K_1
$\tilde{F}_2$

(a)

FIG.1

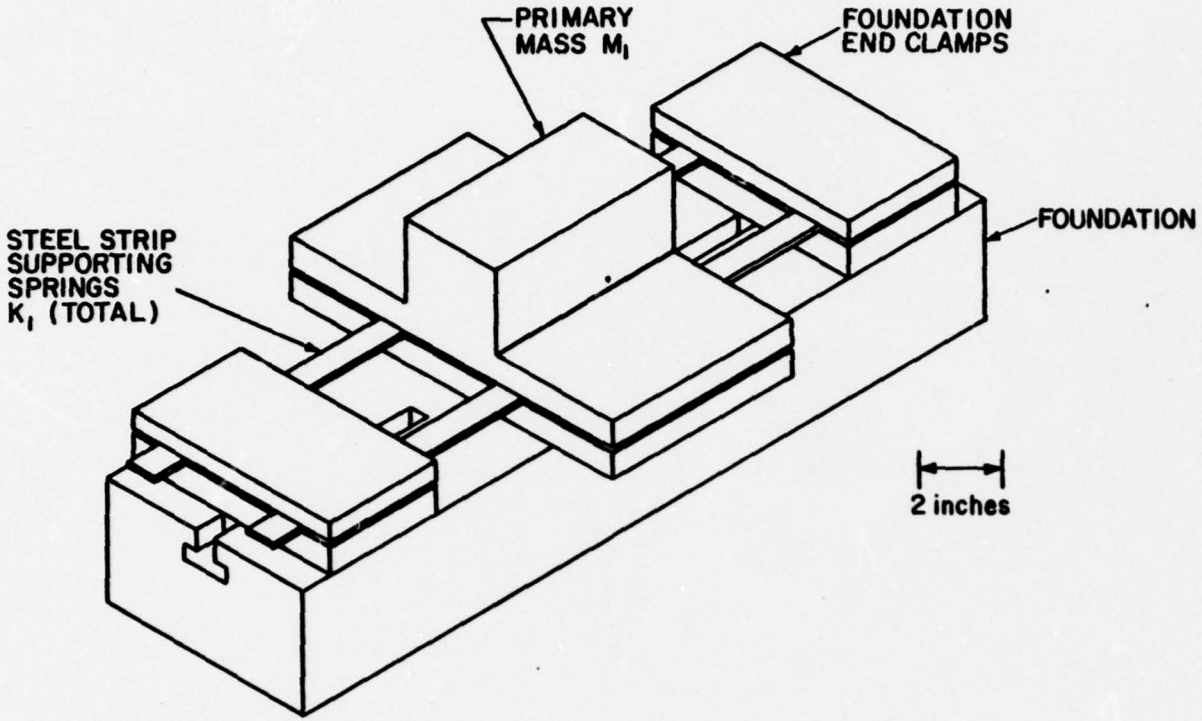
PRIMARY
MASS M_1
FOUNDATION
END CLAMPS
FOUNDATION
STEEL STRIP
SUPPORTING
SPRINGS
K_1 (TOTAL)
2 inches

FIG. 2

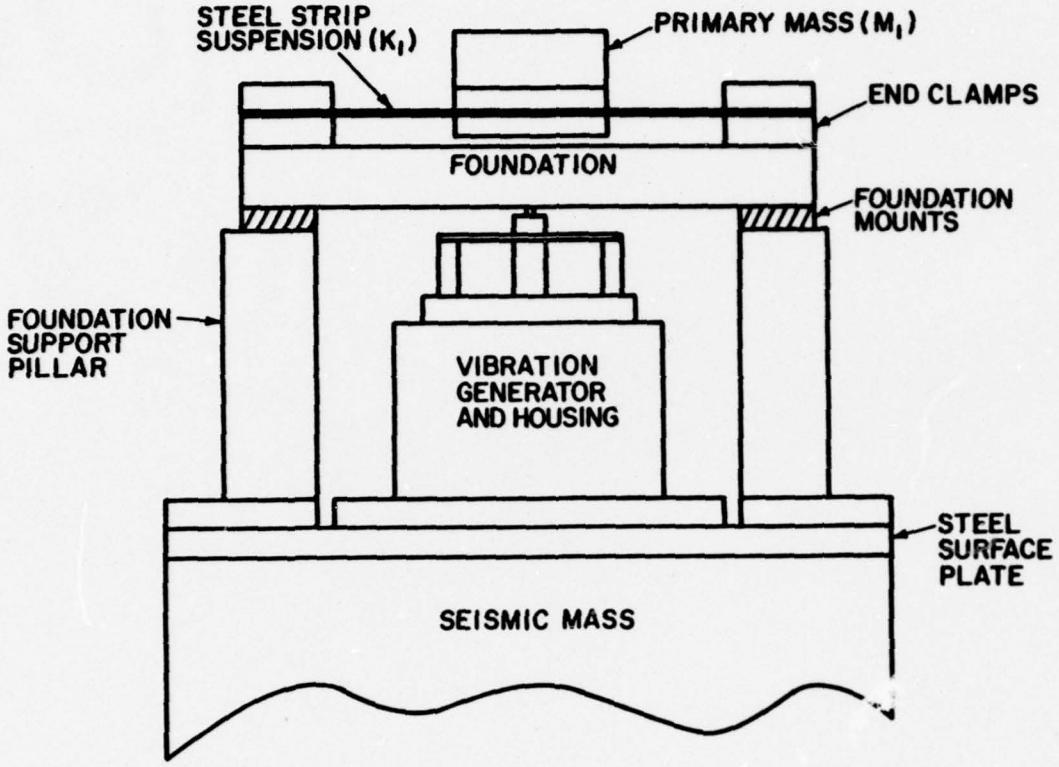
STEEL STRIP
SUSPENSION (K_1)
PRIMARY MASS (M_1)
END CLAMPS
FOUNDATION
FOUNDATION
MOUNTS
FOUNDATION
SUPPORT
PILLAR
VIBRATION
GENERATOR
AND HOUSING
STEEL
SURFACE
PLATE
SEISMIC MASS

FIG. 3

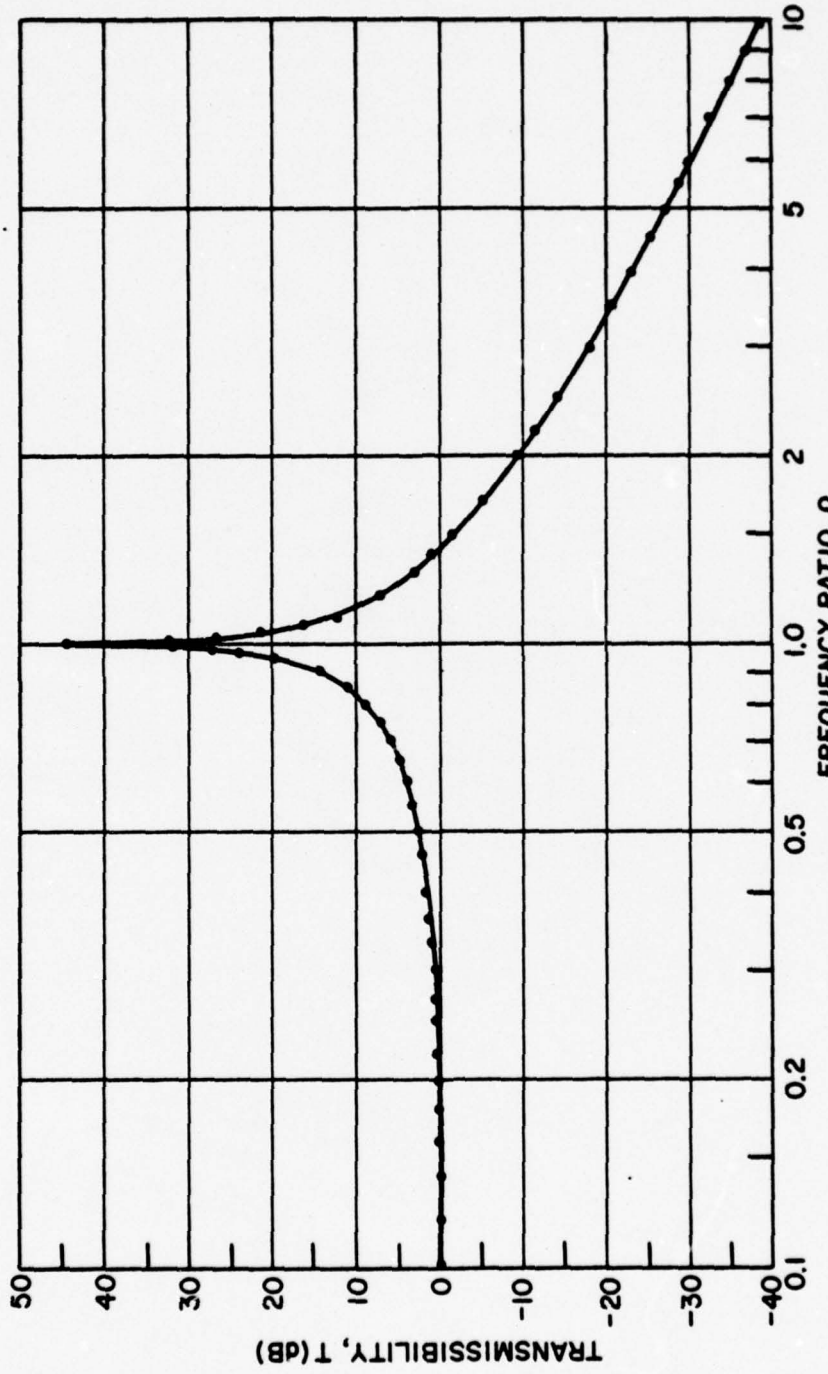
TRANSMISSIBILITY, T (dB)
50
40
30
20
10
0
-10
-20
-30
-40
0.1
0.2
0.5
1.0
2
5
10
FREQUENCY RATIO, Ω

FIG. 4

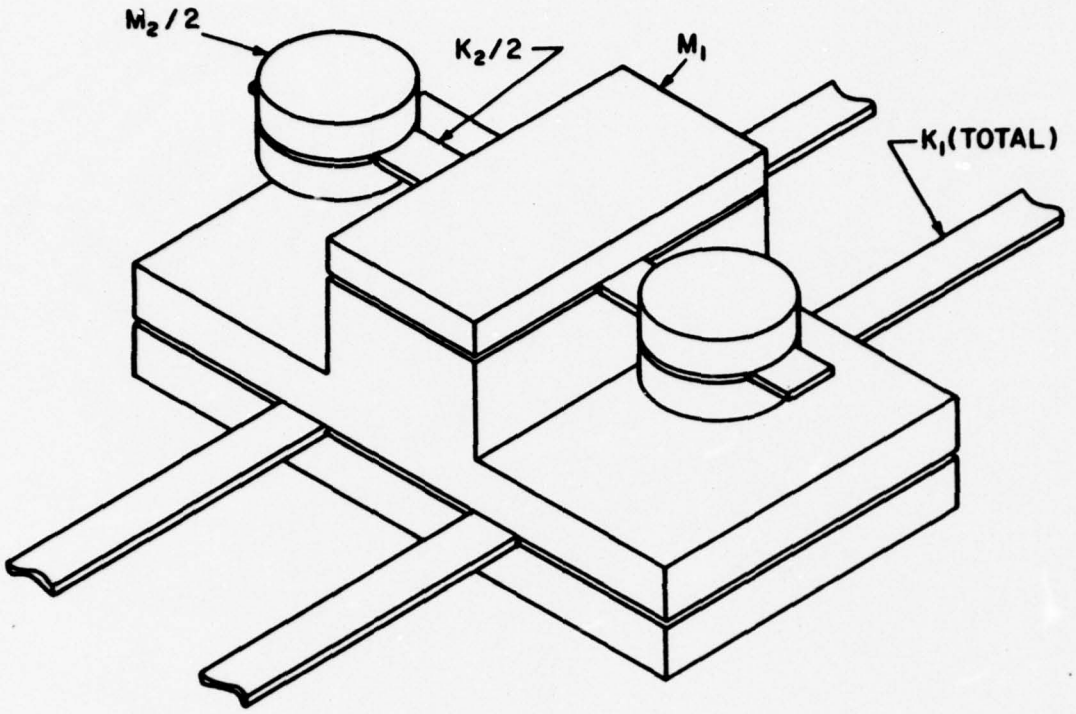

FIG. 5(a)

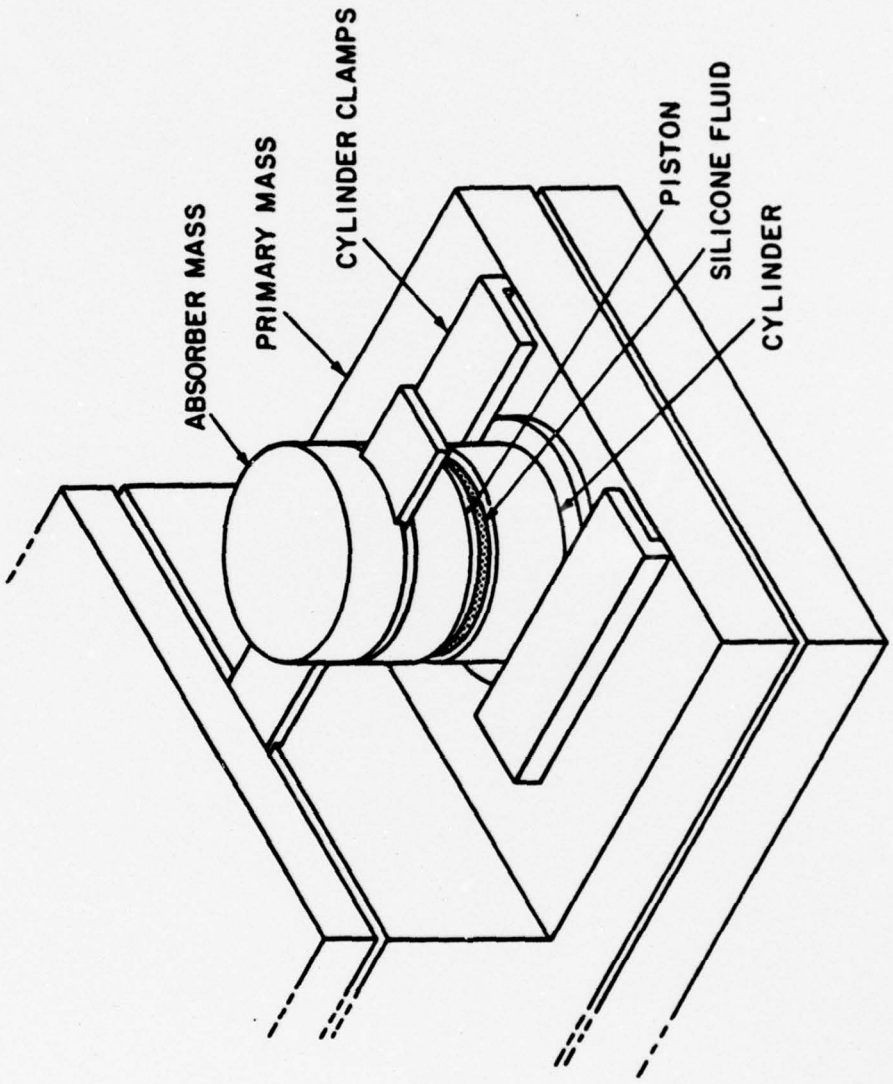
ABSORBER MASS
PRIMARY MASS
CYLINDER CLAMPS
PISTON
SILICONE FLUID
CYLINDER

FIG. 5(b)

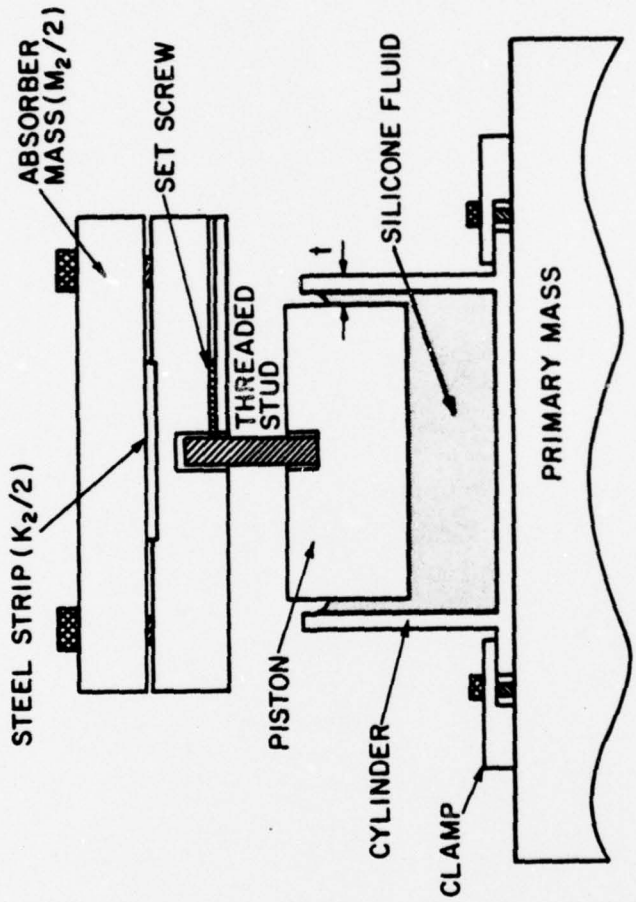
ABSORBER MASS ($M_2/2$)
SET SCREW
STEEL STRIP ($K_2/2$)
THREADED STUD
t
SILICONE FLUID
PISTON
CYLINDER
CLAMP
PRIMARY MASS

FIG. 5(c)

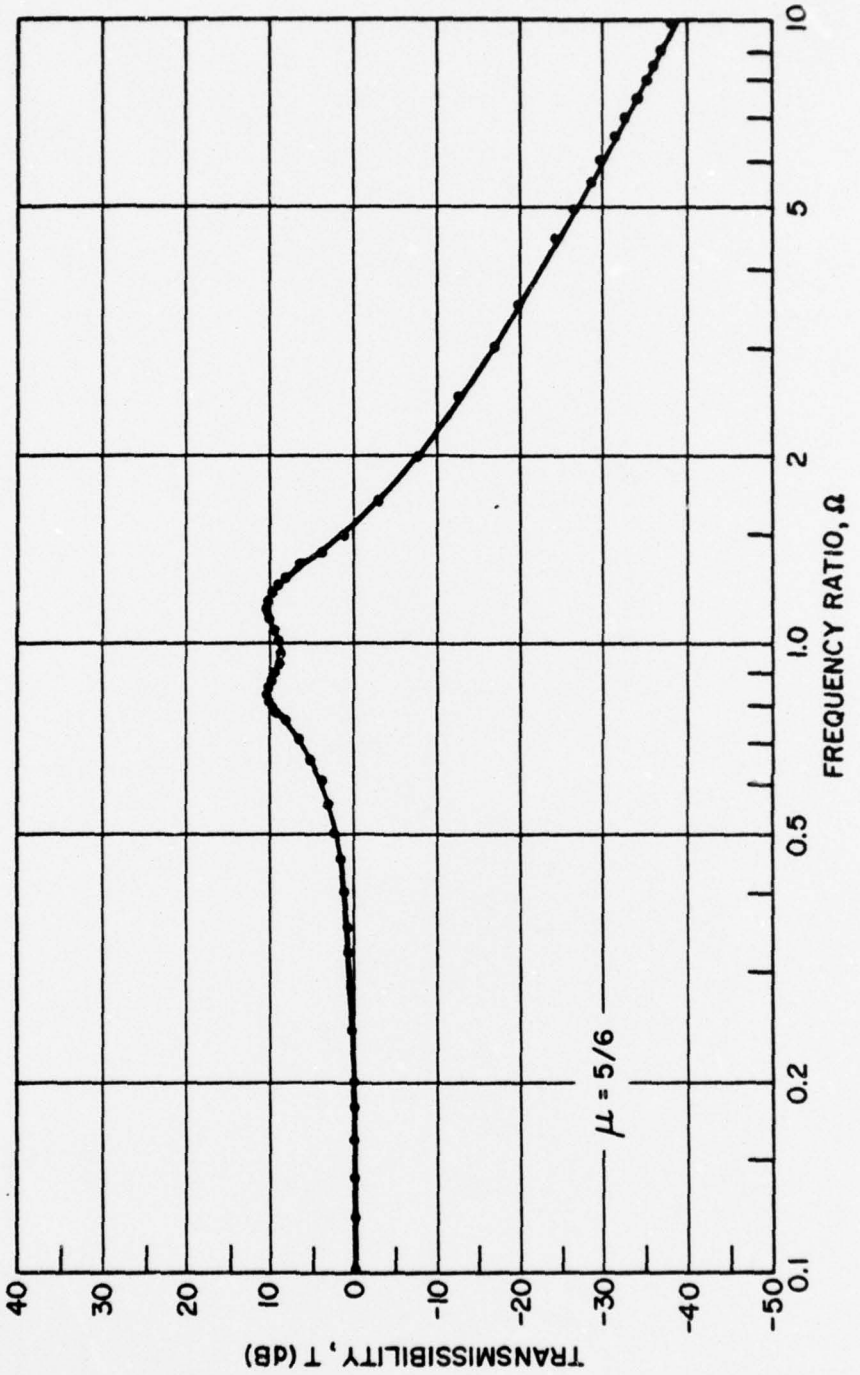
TRANSMISSIBILITY, T (dB)
40
30
20
10
0
-10
-20
-30
-40
-50
0.1
0.2
0.5
1.0
2
5
10
FREQUENCY RATIO, Ω
μ = 5/6

FIG.6

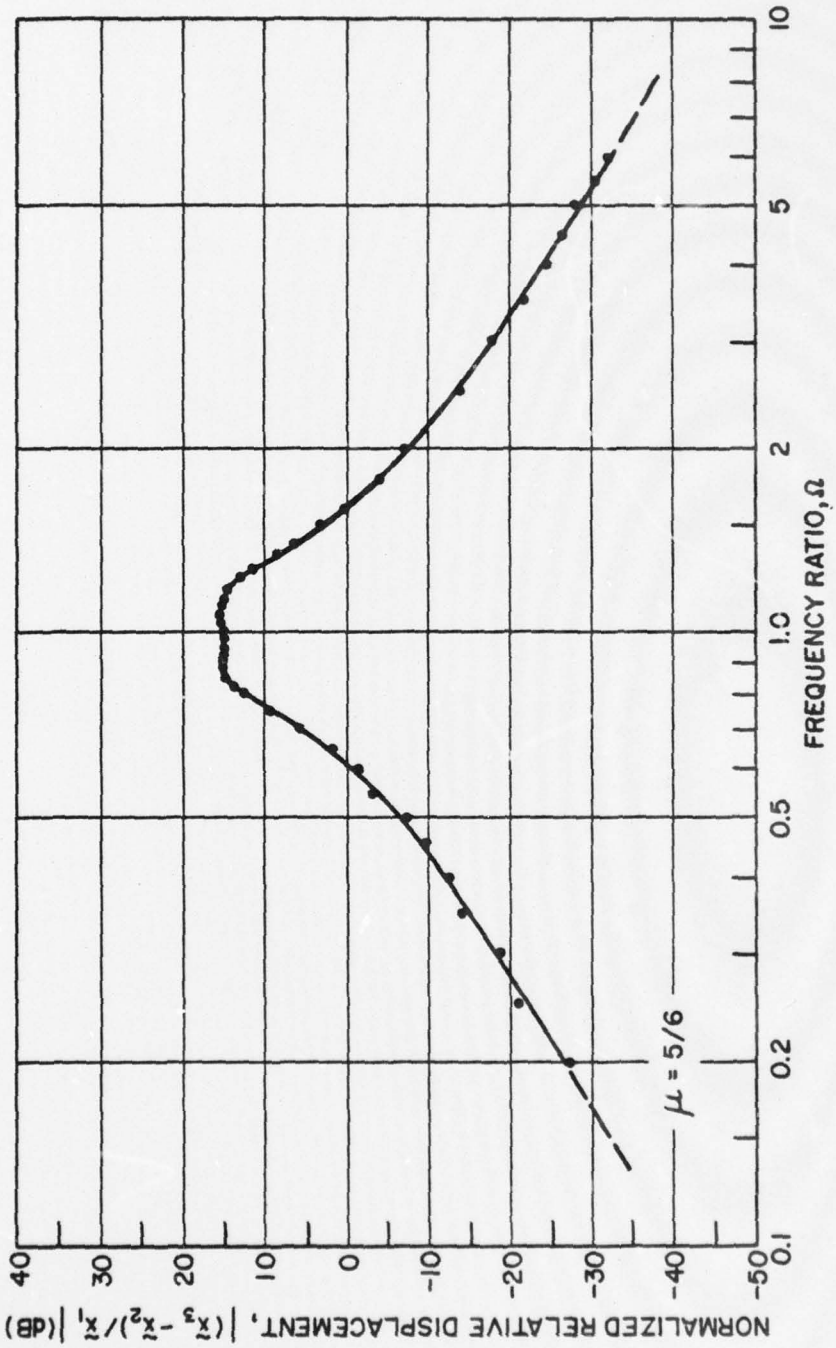
NORMALIZED RELATIVE DISPLACEMENT, $|(\tilde{x}_3 - \tilde{x}_2)/\tilde{x}_1|$ (dB)
40
30
20
10
0
-10
-20
-30
-40
-50
0.1
0.2
0.5
1.0
2
5
10
FREQUENCY RATIO, Ω
$\mu = 5/6$

FIG. 7

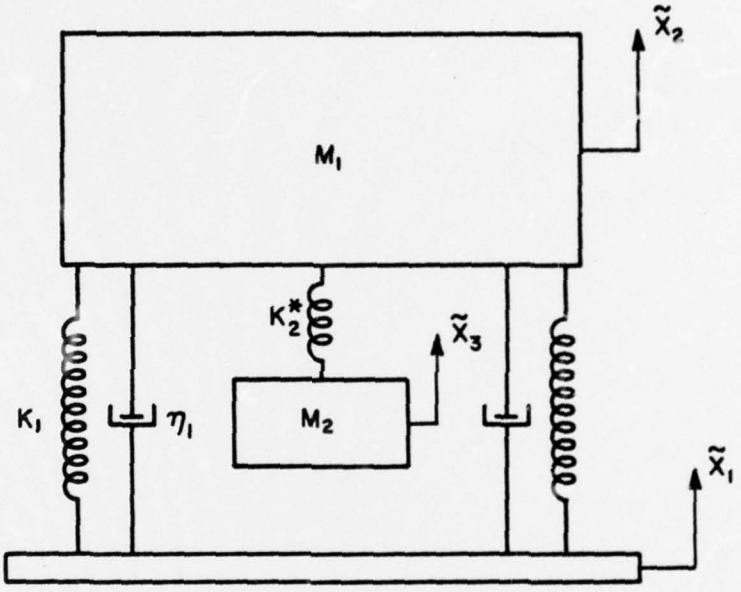

FIG. 8(a)

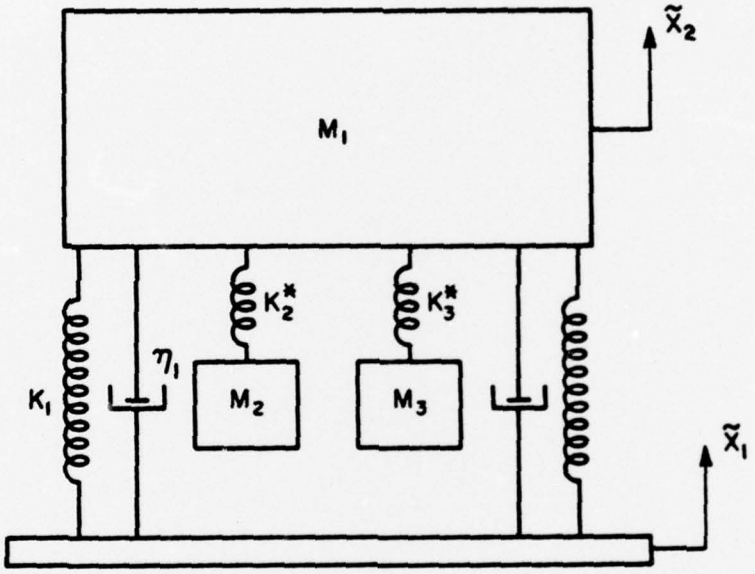

FIG. 8(b)

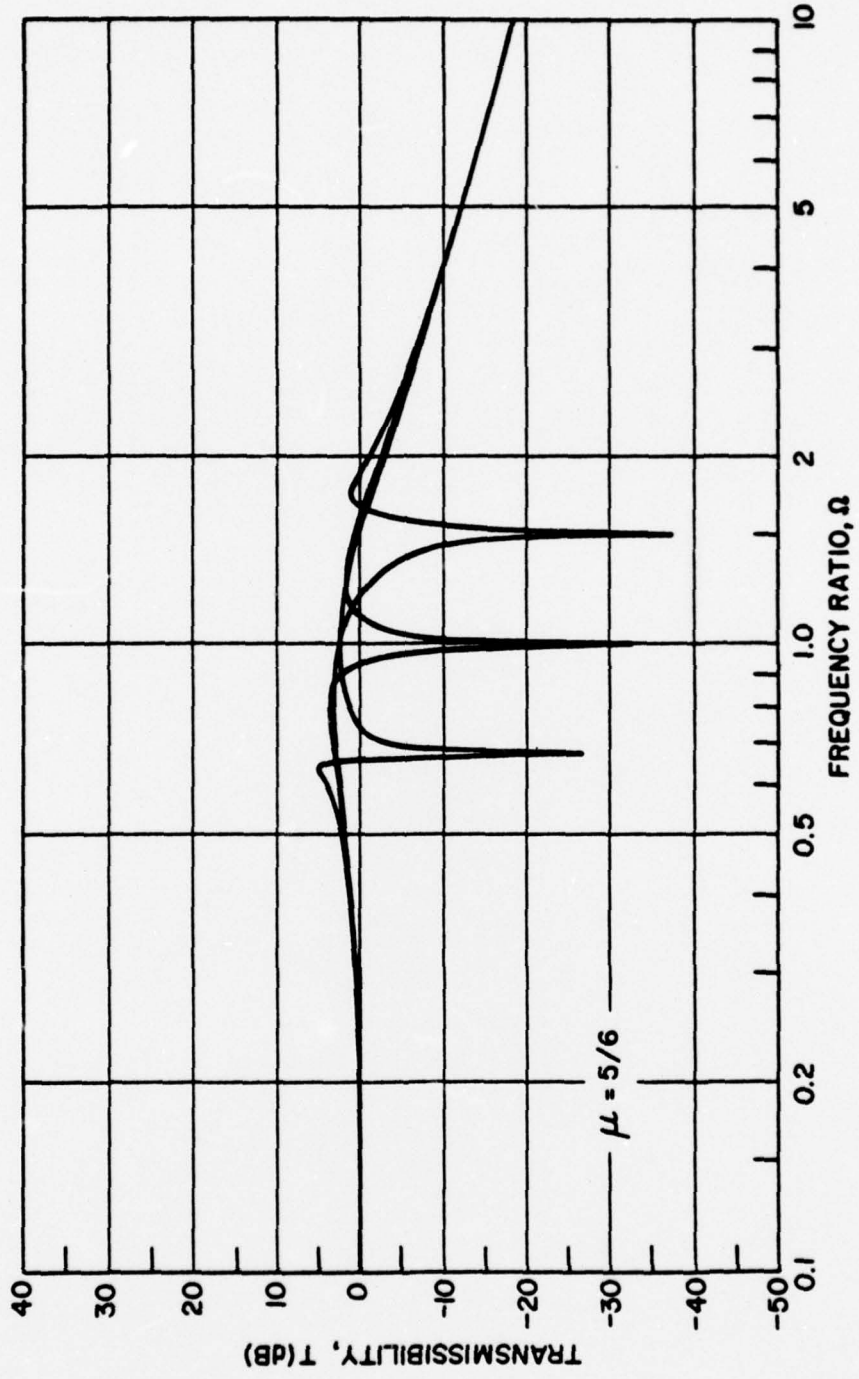
TRANSMISSIBILITY, T(dB)
40
30
20
10
0
-10
-20
-30
-40
-50
0.1
0.2
0.5
1.0
2
5
10
FREQUENCY RATIO, Ω
μ = 5/6

FIG. 9

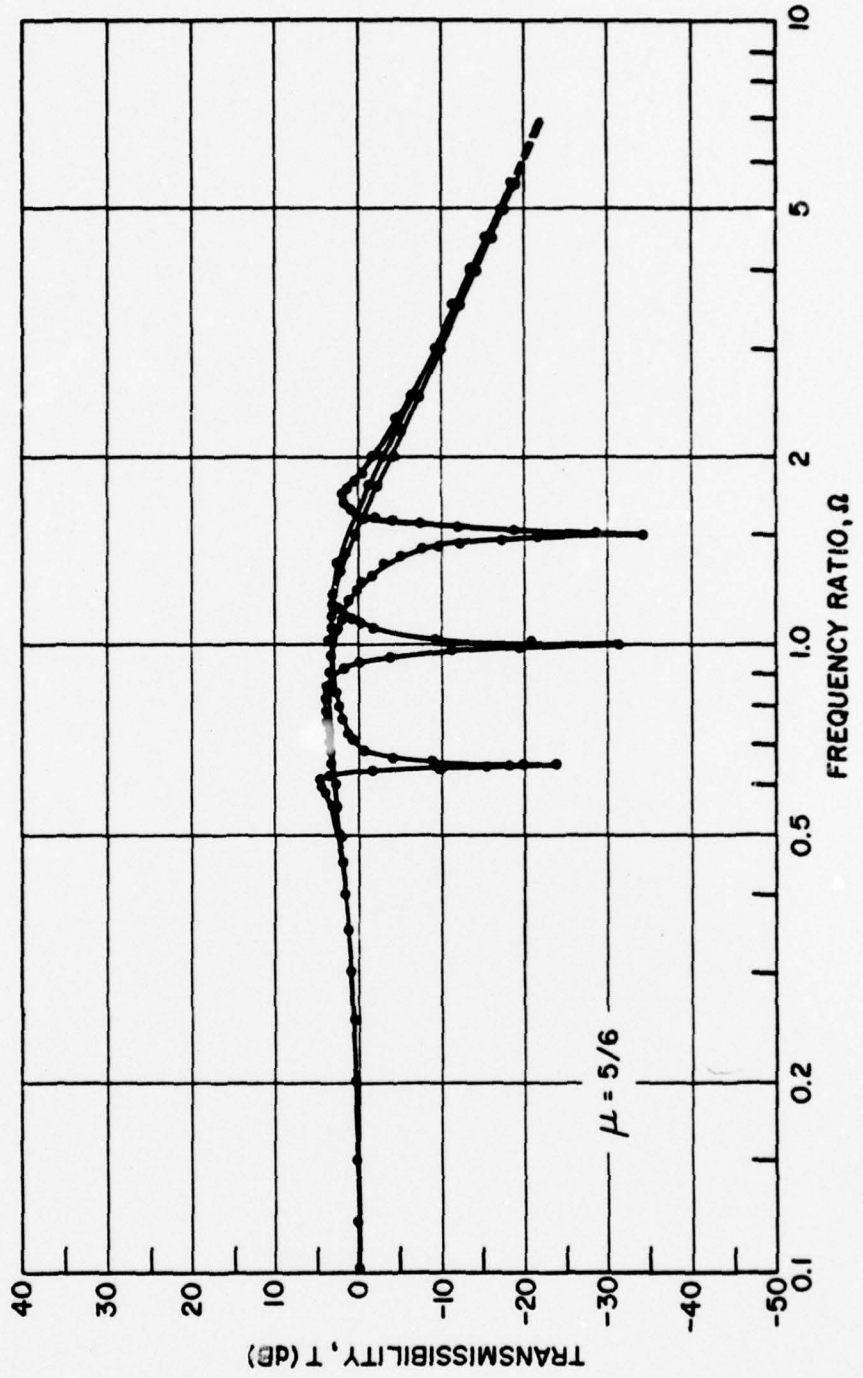
TRANSMISSIBILITY, T (dB)
40
30
20
10
0
-10
-20
-30
-40
-50
0.1
0.2
0.5
1.0
2
5
10
FREQUENCY RATIO, Ω
μ = 5/6

FIG.10

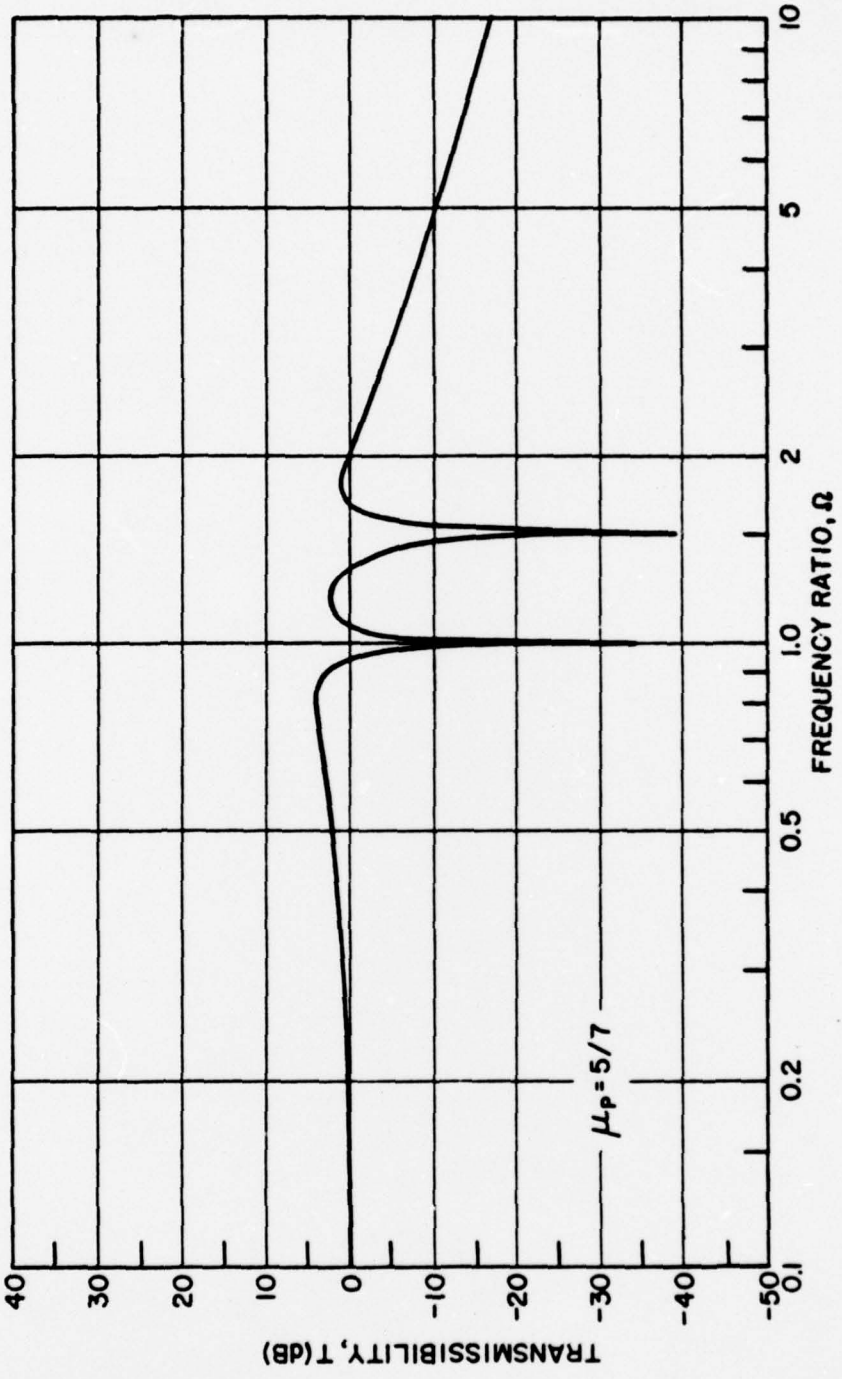
TRANSMISSIBILITY, T(dB)
40
30
20
10
0
-10
-20
-30
-40
-50
0.1
0.2
0.5
1.0
2
5
10
FREQUENCY RATIO, Ω
$\mu_p = 5/7$

FIG.11

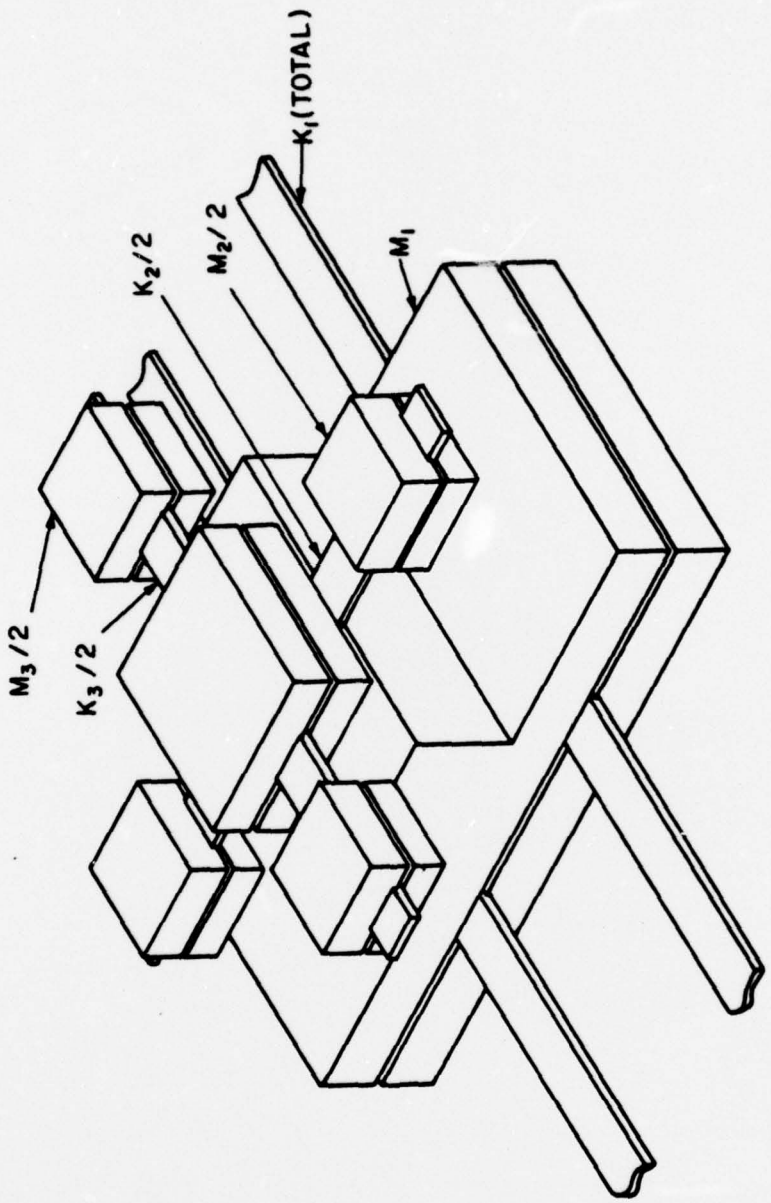

FIG.12

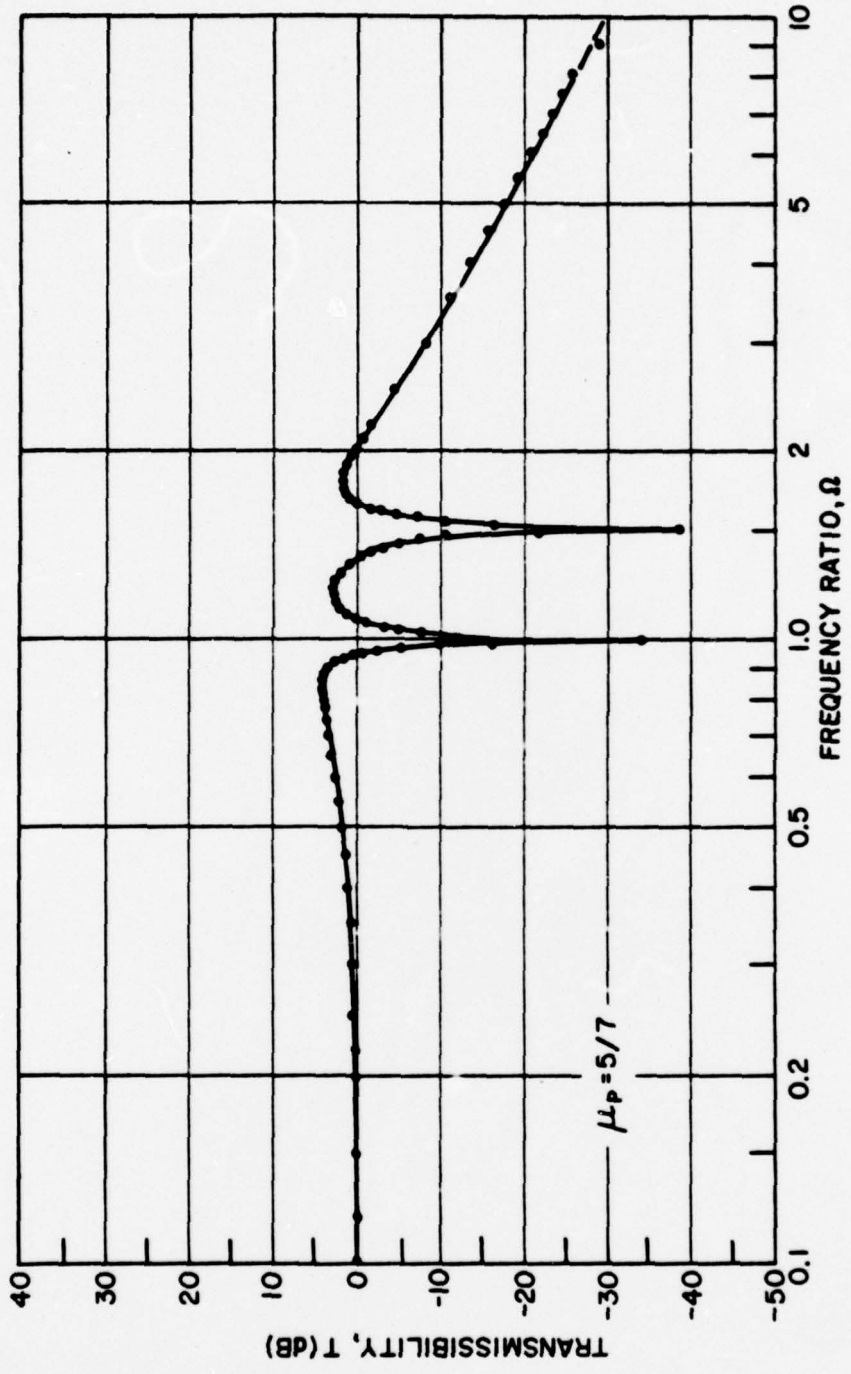
TRANSMISSIBILITY, T (dB)
40
30
20
10
0
-10
-20
-30
-40
-50
0.1
0.2
0.5
1.0
2
5
10
FREQUENCY RATIO, Ω
$\mu_p = 5/7$

FIG.13

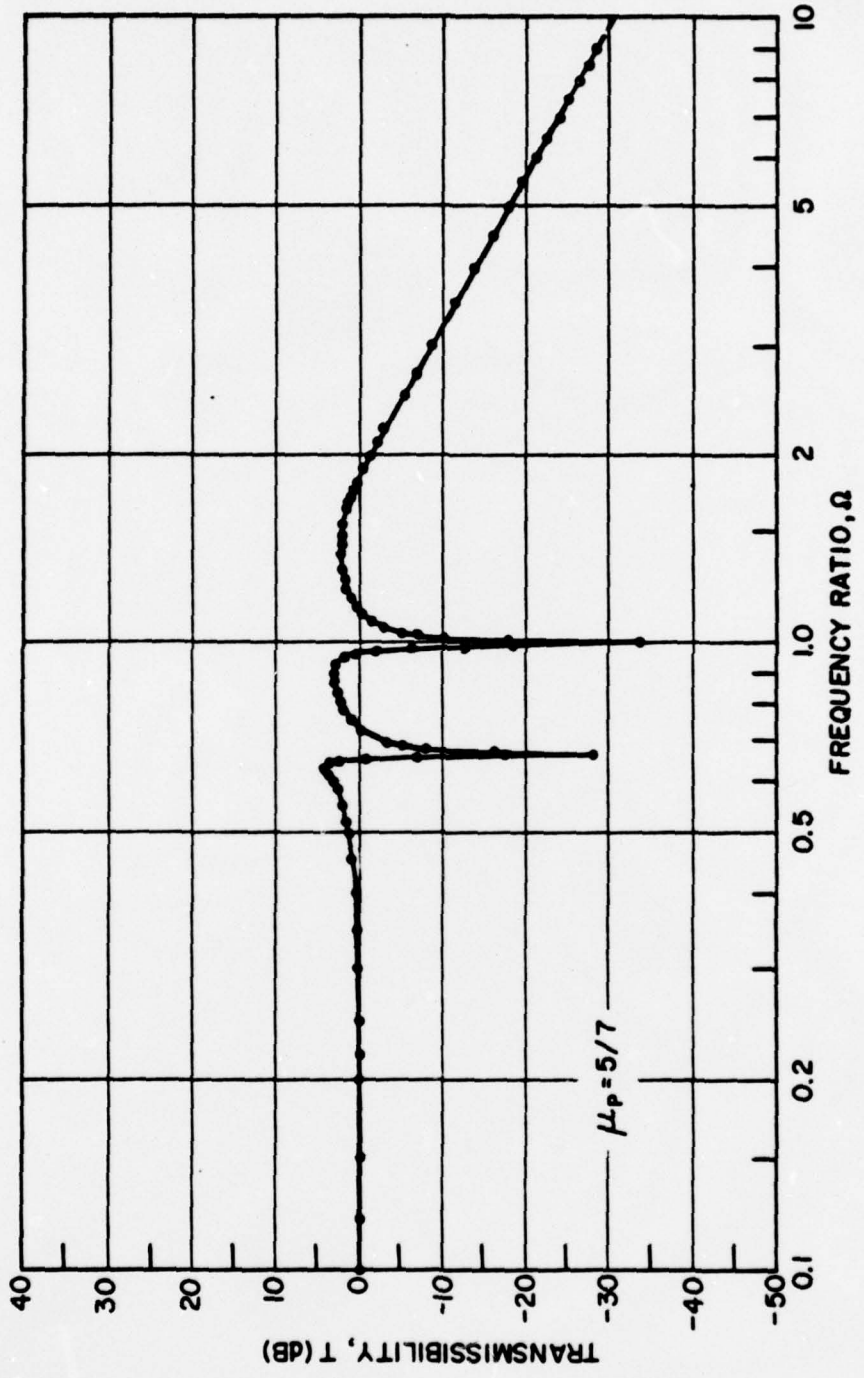
TRANSMISSIBILITY, T (dB)
40
30
20
10
0
-10
-20
-30
-40
-50
0.1
0.2
0.5
1.0
2
5
10
FREQUENCY RATIO, Ω
$\mu_p = 5/7$

FIG.14

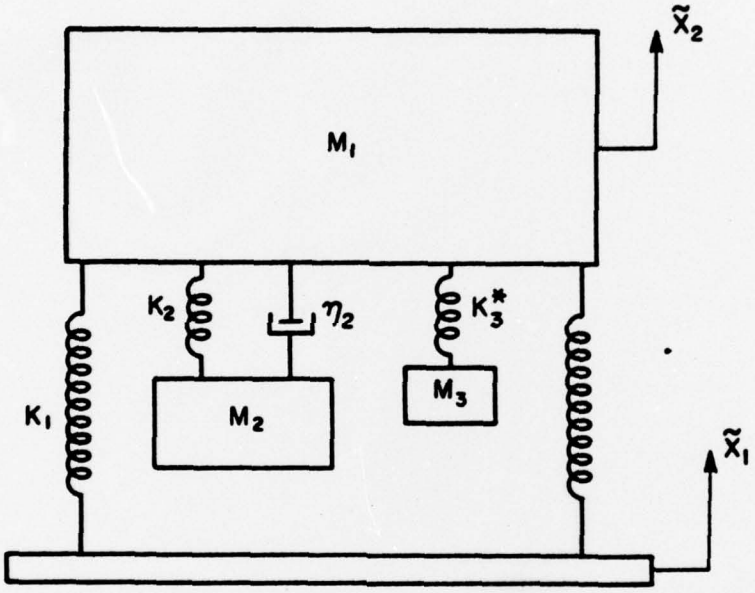

FIG.15

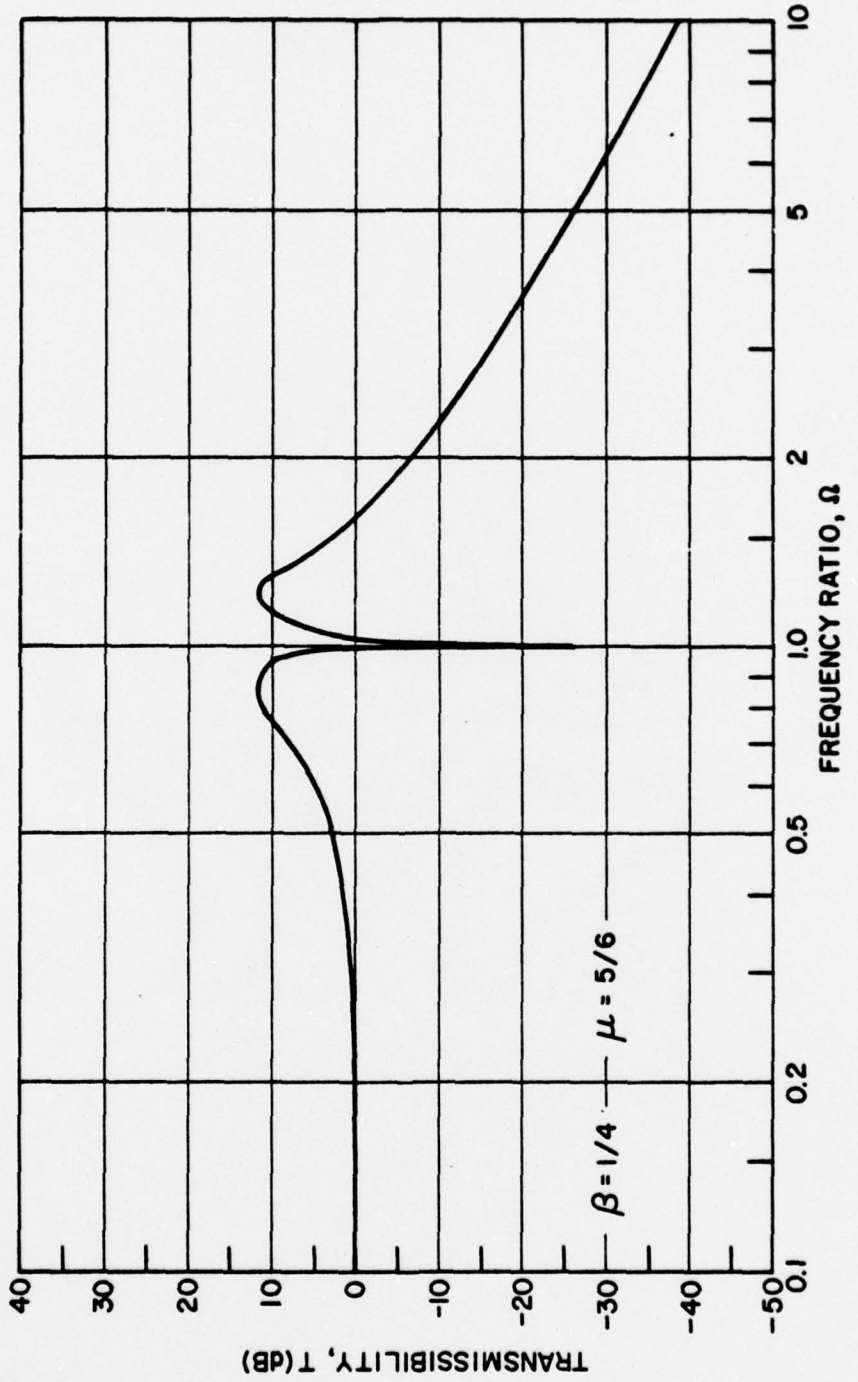
TRANSMISSIBILITY, T (dB)
40
30
20
10
0
-10
-20
-30
-40
-50
0.1
0.2
0.5
1.0
2
5
10
FREQUENCY RATIO, Ω
β = 1/4
μ = 5/6

FIG. 16

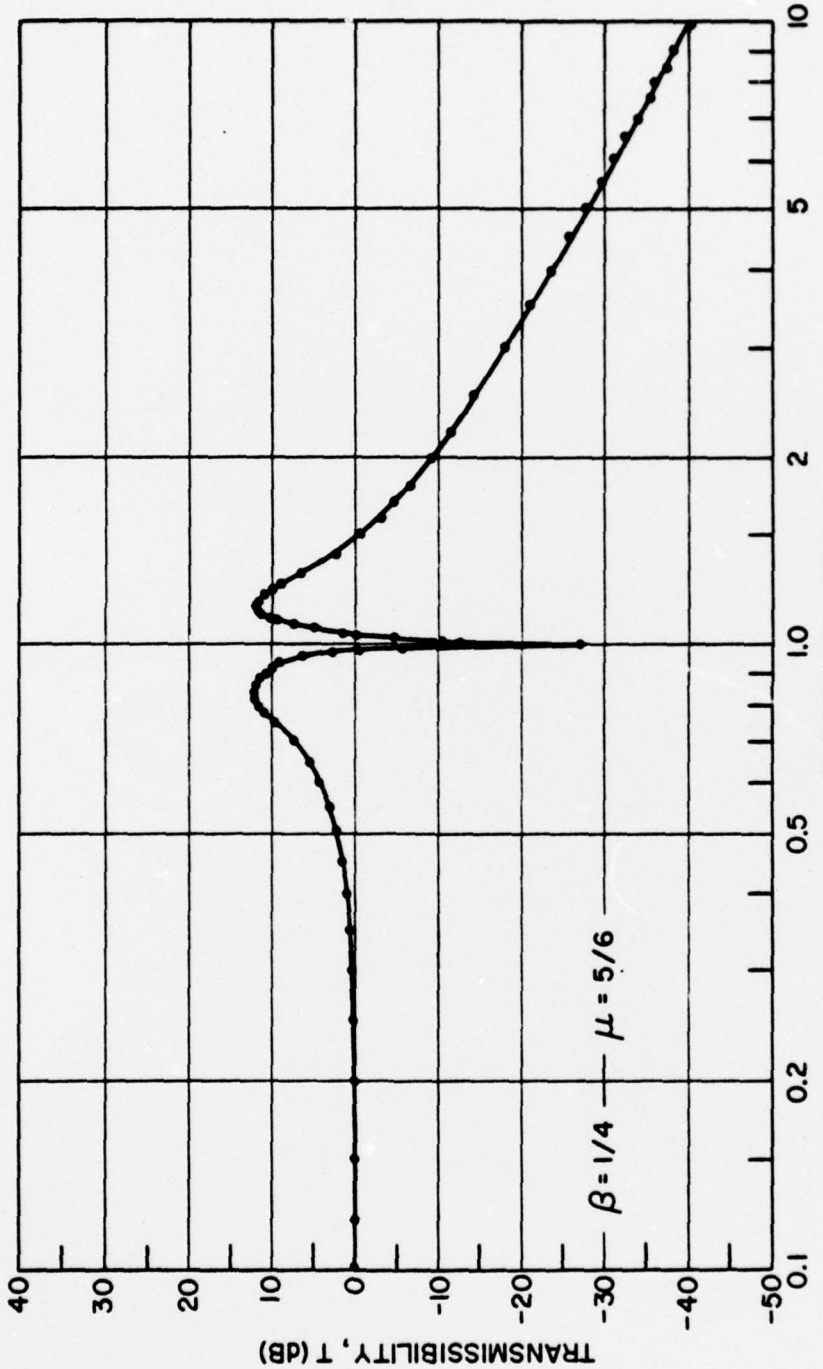
TRANSMISSIBILITY, T (dB)
40
30
20
10
0
-10
-20
-30
-40
-50
0.1
0.2
0.5
1.0
2
5
10
FREQUENCY RATIO, Ω
β = 1/4
μ = 5/6

FIG.17